MODELING TRAVEL-TIME CORRELATIONS BASED ON SENSITIVITY KERNELS AND CORRELATED VELOCITY ANOMALIES

William L. Rodi[1] and Stephen C. Myers[2]

Massachusetts Institute of Technology[1] and Lawrence Livermore National Laboratory[2]

Sponsored by National Nuclear Security Administration
Office of Nonproliferation Research and Development
Office of Defense Nuclear Nonproliferation

Contract No. DE-FC52-05NA26603[1] and W-7405-ENG-48[2]

ABSTRACT

A major contributor to the error in regional and teleseismic event locations is travel-time prediction error, attributable to velocity anomalies in the real Earth that are not represented in the reference Earth model an event locator uses for travel-time calculation. The prediction errors at two stations will, in general, be correlated depending on the spatial coherency of the velocity anomalies compared to the distance between the stations. The motivation for this project is the observation by previous workers that large event location errors can be induced when prediction error correlations are ignored and the observing network of stations is far from uniform. Recently, event location algorithms have been generalized to accept a non-diagonal covariance matrix for data errors as a mechanism for accommodating correlated errors in travel-time predictions. Our project is addressing what to input for the covariance matrix, based on considerations of seismic wave propagation and the statistical characterization of the Earth's velocity heterogeneity. Specifically, we are developing numerical algorithms that generate a travel-time covariance matrix for a network of stations, as a function of the event location, by integrating a velocity covariance function, as defined in geostatistical analysis, with the travel-time sensitivity kernels appropriate for the event-station paths. This paper describes two alternative techniques for performing this calculation, which are compared in a numerical example. A second example of our approach investigates the variation of travel-time variances and correlations over regional and near-teleseismic distances, computed using ray sensitivities for a 1D reference Earth model. This example demonstrates a strong dependence on ray parameter that agrees qualitatively with empirical observations.

Report Documentation Page

Form Approved
OMB No. 0704-0188

1. REPORT DATE	2. REPORT TYPE	3. DATES COVERED
SEP 2007		**00-00-2007 to 00-00-2007**

4. TITLE AND SUBTITLE	5a. CONTRACT NUMBER
Modeling Travel-Time Correlations Based on Sensitivity Kernels and Correlated Velocity Anomalies	5b. GRANT NUMBER
	5c. PROGRAM ELEMENT NUMBER
6. AUTHOR(S)	5d. PROJECT NUMBER
	5e. TASK NUMBER
	5f. WORK UNIT NUMBER
7. PERFORMING ORGANIZATION NAME(S) AND ADDRESS(ES) **Lawrence Livermore National Laboratory,PO Box 808,Livermore,CA,94551-0808**	8. PERFORMING ORGANIZATION REPORT NUMBER
9. SPONSORING/MONITORING AGENCY NAME(S) AND ADDRESS(ES)	10. SPONSOR/MONITOR'S ACRONYM(S)
	11. SPONSOR/MONITOR'S REPORT NUMBER(S)

12. DISTRIBUTION/AVAILABILITY STATEMENT
Approved for public release; distribution unlimited

13. SUPPLEMENTARY NOTES
Proceedings of the 29th Monitoring Research Review: Ground-Based Nuclear Explosion Monitoring Technologies, 25-27 Sep 2007, Denver, CO sponsored by the National Nuclear Security Administration (NNSA) and the Air Force Research Laboratory (AFRL)

14. ABSTRACT
see report

15. SUBJECT TERMS

16. SECURITY CLASSIFICATION OF:			17. LIMITATION OF ABSTRACT	18. NUMBER OF PAGES	19a. NAME OF RESPONSIBLE PERSON
a. REPORT **unclassified**	b. ABSTRACT **unclassified**	c. THIS PAGE **unclassified**	**Same as Report (SAR)**	**9**	

OBJECTIVE

To achieve accurate event locations and estimates of location uncertainty, seismic event location algorithms must account for two types of errors: *pick* errors in the measured arrival times of the seismic phases observed at various stations, and *model* errors incurred in predicting travel time for the observed station/phase combinations as a function of the event location. Model errors are attributable to velocity anomalies in the Earth that are not rendered in the velocity model used for travel-time prediction. When the observing stations are sufficiently close to one another, their model errors are expected to be correlated. While it is now standard practice for event location algorithms used in nuclear monitoring to assign error *variances* that include the contribution from model prediction errors, the algorithms generally set the error *covariances* to zero; correlations are ignored. Doing so can seriously degrade location accuracy when the distribution of seismic stations is far from uniform (e.g. Chang et al., 1983; Yang et al. 2004).

This project is investigating the phenomenon of correlated travel-time prediction errors from a physical point of view, making use of the principles of wave propagation through heterogeneous media and our knowledge of the statistical properties of the Earth's heterogeneity. Specifically, we are developing techniques to calculate covariance matrices of travel-time model errors by integrating travel-time sensitivity kernels with plausible correlation functions describing the Earth's velocity heterogeneity. Our preliminary efforts in this development were reported by Rodi and Myers (2006). Here we summarize our approach and report on our recent efforts.

RESEARCH ACCOMPLISHED

Formulation of Approach

Given a set of n arrival time data from an event, one can decompose the data errors as (for $i = 1,\ldots,n$)

$$\mathrm{e}_i = e_{\mathrm{p},i} + \mathrm{e}_{\mathrm{m},i}, \tag{1}$$

where the first term is the *pick*, or measurement, error and the second term is the *model* error, or error in the travel-time prediction from a reference Earth velocity model. Typically, event location algorithms assume that the variances assigned to the arrival time data, σ_i^2, include a contribution for each type of error:

$$\sigma_i^2 = \sigma_{\mathrm{p},i}^2 + \sigma_{\mathrm{m},i}^2. \tag{2}$$

However, the errors for different i are assumed uncorrelated. We are addressing the problem of calculating a full covariance matrix for model errors, having components $\sigma_{\mathrm{m},ij}$ defined by

$$\sigma_{\mathrm{m},ij} = \mathrm{E}[e_{\mathrm{m},i}\, e_{\mathrm{m},j}]. \tag{3}$$

E[ ] denotes the expectation operator.

To explain our approach to covariance modeling, we consider only P-wave arrivals. Let $v_0(\mathbf{x})$ denote the P velocity function for the reference model, and $v_E(\mathbf{x})$ denote the Earth's true (and unknown) velocity function. Then, model errors can be linked to the slowness difference, which we denote $m(\mathbf{x})$:

$$m(\mathbf{x}) = v_E^{-1}(\mathbf{x}) - v_0^{-1}(\mathbf{x}). \tag{4}$$

We assume that the travel-time dependence on slowness can be adequately approximated as linear, allowing us to express the model error in the ith datum as

$$e_{\mathrm{m},i} = \int a_i(\mathbf{x})\, m(\mathbf{x})\, d\mathbf{x}\,, \tag{5}$$

where $a_i(\mathbf{x})$ is the first-order sensitivity kernel of the ith travel-time functional, as evaluated at v_0. In the high-frequency limit, this kernel is concentrated along the geometrical ray connecting the event and station

locations. For finite frequency, it is spatially distributed around this ray. In either case, we point out that the model error is a function of the event *and* station locations.

We consider $m(\mathbf{x})$ to be a Gaussian random field, having zero mean and a specified covariance between any two points, described by a covariance operator $C(\mathbf{x},\mathbf{x}')$:

$$\mathrm{E}\left[m(\mathbf{x})\right] = 0 \tag{6}$$

$$E\left[m(\mathbf{x})m(\mathbf{x}')\right] = C(\mathbf{x},\mathbf{x}'). \tag{7}$$

The covariance between two model errors is then given by

$$\sigma_{\mathrm{m},ij} = \int d\mathbf{x}\, a_i(\mathbf{x}) \int d\mathbf{x}'\, C(\mathbf{x},\mathbf{x}')\, a_j(\mathbf{x}'). \tag{8}$$

Equation (8) implies that the extent to which two model errors are correlated depends on the spatial relationship between their sensitivity kernels in relation to the correlation structure of the velocity field.

Velocity Model Covariance Operators

When $m(\mathbf{x})$ is a stationary random field, $C(\mathbf{x},\mathbf{x}')$ depends only on the difference between the points $\mathbf{x}$ and $\mathbf{x}'$. For example, if $m(\mathbf{x})$ is isotropic with a *correlation function* of the exponential type (Deutsch and Journel, 1998), then

$$C(\mathbf{x},\mathbf{x}') = \sigma^2 \exp\left[-\frac{|\mathbf{x}-\mathbf{x}'|}{\lambda}\right], \tag{9}$$

where σ^2 is the variance of the slowness field and λ is a correlation length. However, the Earth's velocity heterogeneity is not well-approximated as stationary over the spatial scales affecting regional and teleseismic waves. It is difficult to generalize an operator such as the exponential form above to allow for nonstationarity while preserving the essential properties of $C(\mathbf{x},\mathbf{x}')$, in particular its being a positive-definite operator.

A flexible approach to characterizing nonstationary random fields is to specify the covariance operator indirectly through its operator inverse, which we denote *D*, such that

$$DC(\mathbf{x},\mathbf{x}') = \delta(\mathbf{x}-\mathbf{x}'). \tag{10}$$

If we take *D* to be a differential operator, then $C(\mathbf{x},\mathbf{x}')$ is its Green's function. Rodi et al. (2003) implemented this approach with *D* as

$$D = \frac{\mathrm{const}}{\lambda_1^2\lambda_2\sigma^2}\left[\delta(\mathbf{x}) - \frac{1}{(2l-3)}\left(\frac{\lambda_1^2}{r^2}\nabla_1^2 + \lambda_2^2\frac{\partial^2}{\partial z^2}\right)\right]^l, \quad l \geq 2. \tag{11}$$

Here, *l* is an integer specifying the order of the operator; ∇_1^2 is the horizontal Laplacian operator; λ_1 and λ_2 are horizontal and vertical correlation lengths, respectively; and σ^2 is the variance. The exponential-type covariance operator of equation (9) is given by $l = 2$, ignoring boundaries.

In previous work (Rodi and Myers, 2006) we have implemented our numerical algorithms for covariance modeling with *D* being nonstationary only by virtue of the boundary at the Earth's surface and velocity discontinuities (e.g., the Moho), across which $C(\mathbf{x},\mathbf{x}')$ is allowed to "de-correlate", i.e. $C(\mathbf{x},\mathbf{x}') = 0$ when $\mathbf{x}$ and $\mathbf{x}'$ are on opposing sides of the discontinuity. One of the accomplishments of the current year has been to implement a more general form of nonstationarity whereby σ and λ_2 (vertical correlation distance) are allowed to vary with depth.

Covariance Modeling Algorithms

The numerical techniques we have developed apply to a discrete model parameterization. We thus replace the model function $m(\mathbf{x})$ with a $k \times 1$ vector $\mathbf{m}$; the sensitivity kernels $a_i(\mathbf{x})$ with $k \times 1$ vectors $\mathbf{a}_i$; and the operators C and D with $k \times k$ matrices $\mathbf{C}$ and $\mathbf{D}$. We require that

$$\mathbf{DC} = \mathbf{I}, \tag{12}$$

where $\mathbf{I}$ is the $k \times k$ identity matrix.

In the discrete formulation, the double integral of equation (8) becomes the quadratic matrix expression

$$\sigma_{\mathrm{m},ij} = \mathbf{a}_i^T \mathbf{C} \mathbf{a}_j . \tag{13}$$

It is also useful to express the full $n \times n$ model-error covariance matrix, which we denote $\mathbf{V}_\mathrm{m}$ and whose elements are the $\sigma_{\mathrm{m},ij}$. To do this, we first define the $n \times k$ sensitivity matrix having the sensitivity vectors as its rows:

$$\mathbf{A}^T = \left(\mathbf{a}_1 \;\; \mathbf{a}_2 \;\; \cdots \;\; \mathbf{a}_n \right). \tag{14}$$

We can then write

$$\mathbf{V}_\mathrm{m} = \mathbf{ACA}^T . \tag{15}$$

We now outline two numerical methods we have developed for computing $\mathbf{V}_\mathrm{m}$. Both assume that $\mathbf{D}$ is specified directly, with $\mathbf{C}$ then being given implicitly as the inverse of $\mathbf{D}$. Both methods require that the sensitivity vectors, $\mathbf{a}_i$, be given explicitly.

Explicit Method

This method entails solving a linear system for each j, given by

$$\mathbf{Du}_j = \mathbf{a}_j. \tag{16}$$

Given the solution vector $\mathbf{u}_j$, the elements of one column of the model-error covariance matrix can be found as

$$\sigma_{\mathrm{m},ij} = \mathbf{a}_i^T u_j , \qquad i = 1, \ldots, n \tag{17}$$

since, analytically, $\mathbf{u}_j = \mathbf{Ca}_j$. Repeating for each $j = 1,\ldots,n$, the full matrix $\mathbf{V}_\mathrm{m}$ is generated.

Being an approximation to a differential operator, the matrix $\mathbf{D}$ is highly sparse. Therefore, our implementation of this method solves (16) with a conjugate gradients technique.

Theoretically, the matrix obtained with the explicit method will be symmetric since $\mathbf{u}_i^T \mathbf{a}_j = \mathbf{u}_j^T \mathbf{a}_i$ if the solution vectors $\mathbf{u}_j$ are exact. Numerically, however, this will not be the case exactly. Therefore, we average the two numerical estimates of $\sigma_{\mathrm{m}ij}$ $(i \neq j)$ to generate a symmetric approximation to $\mathbf{V}_\mathrm{m}$.

Implicit Method

This method was described by Rodi and Myers (2006) and we summarize it here for completeness.

For each j we solve a *minimization* problem for a vector in the model space, $\mathbf{w}_j$:

$$\left(\mathbf{n}_j - \mathbf{A}\mathbf{w}_j \right)^T \mathbf{V}_\mathrm{p}^{-1} \left(\mathbf{n}_j - \mathbf{A}\mathbf{w}_j \right) + \mathbf{w}_j^T \mathbf{D} \mathbf{w}_j = \text{minimum} \tag{18}$$

where $\mathbf{V}_P$ is some assumed, *diagonal* covariance matrix for pick errors, and $\mathbf{n}_j$ is the jth column of the $n \times n$ identity matrix. Again, we compute the solution $\mathbf{w}_j$ with a conjugate gradients technique. Given the solution, we form the residual vector

$$\mathbf{r}_j = \mathbf{n}_j - \mathbf{A}w_j . \tag{19}$$

Repeating this process for each j = 1, …, n, we generate a residual matrix column-by-column:

$$\mathbf{R} = \begin{pmatrix} \mathbf{r}_1 & \mathbf{r}_2 & \cdots & \mathbf{r}_n \end{pmatrix}. \tag{20}$$

Rodi and Myers (2006) showed that

$$\mathbf{R} = \mathbf{V}_p \left(\mathbf{A}\mathbf{C}\mathbf{A}^T + V_p \right)^{-1}. \tag{21}$$

Therefore, two useful quantities can be generated from **R**. The first is the inverse of the *total* covariance matrix:

$$\left(\mathbf{V}_m + V_p \right)^{-1} = V_p^{-1}\mathbf{R}. \tag{22}$$

This matrix can be used by an event location algorithm in the calculation of a misfit function, assuming $\mathbf{V}_P$ is appropriate. Second, we have the object of this project, the model-error covariance matrix:

$$\mathbf{V}_m = \left(\mathbf{V}_p^{-1}\mathbf{R} \right)^{-1} - \mathbf{V}_p . \tag{23}$$

As before, the numerically generated $\mathbf{V}_m$ obtained from this formula is not guaranteed to be symmetric, but we can average it with its transpose to make it so.

For the purpose of calculating $\mathbf{V}_m$ by the implicit method, the matrix $\mathbf{V}_P$ is arbitrary. We have found that setting it to a fraction of the identity yields accurate results. If $\mathbf{V}_P$ is sufficiently small, we can ignore it and directly obtain a third quantity which can be useful in a location algorithm:

$$\mathbf{V}_m^{-1} \approx \mathbf{V}_p^{-1}\mathbf{R}. \tag{24}$$

Comparison of Explicit and Implicit Methods

Rodi and Myers (2006) presented an example of a travel-time (model-error) covariance matrix for a network of 12 regional stations observing a shallow earthquake in northeastern Iran. Figure 1 displays the station geometry for this example. The event comes from the EHB (Engdahl et al., 1998) data base and is one of the events used by Reiter and Rodi (2006) in their body-wave tomography study of southern Asia. The covariance calculations were performed using sensitivity vectors (discretized kernels) generated by Reiter and Rodi (2006) for their initial 3D velocity model, calculated with a finite-difference raytracing technique. The results we show here have been updated using a more recent tomographic model (Rodi and Reiter, 2007) and revised values of geostatistical parameters for the Earth's velocity. Velocity variations were assigned a standard deviation (σ) of 3% in the crust and 1.5% in the upper mantle. The vertical correlation distance (λ_2) in the crust was set to half the crustal thickness, while λ_2 = 60 km was used throughout the upper mantle. The horizontal correlation distance was 300 km in the crust and upper mantle.

We display two aspects of the 12×12 model-error covariance matrices ($\mathbf{V}_m$) resulting from our calculations. Figure 2 displays the 12 standard deviations (square-root of the diagonal elements) as a function of epicentral distance. The 66 independent off-diagonal elements, normalized as correlation coefficients, are plotted as a function of inter-station azimuth in Figure 3. The distance and azimuth dependence of the covariances behave as expected, qualitatively at least validating our modeling approach (see Rodi and Myers, 2006, for a more detailed discussion of the results). For our purposes here, we point out that the two numerical techniques we applied, which are compared in each figure, produce very similar results, although some small difference can be seen.

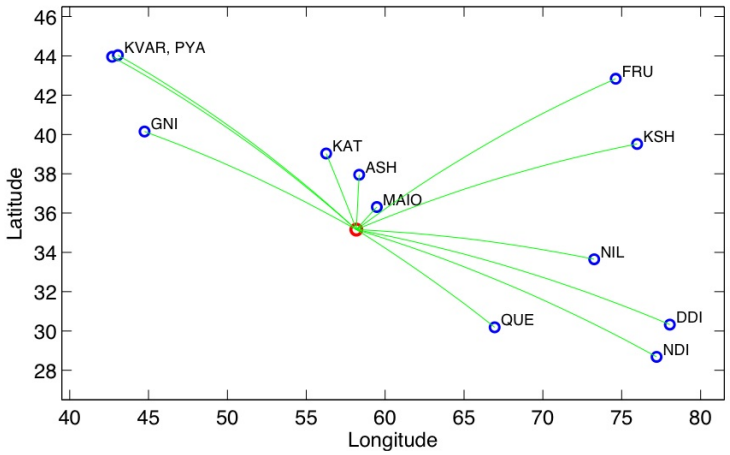

Figure 1. Event/station geometry used for testing our travel-time covariance modeling algorithms. The event epicenter is marked as the red circle. The event had Pn arrivals for 12 stations, marked as blue circles.

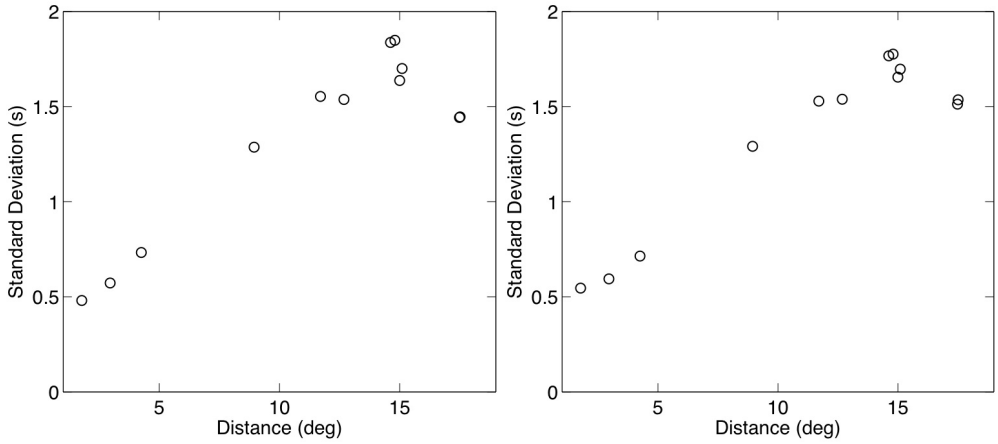

Figure 2. Standard deviation of model error as a function of epicentral distance computed with the explicit method (left) and implicit method (right). The event-station geometry is shown in Figure 1.

Distance Dependence of Travel-Time Covariance

Our second example uses a linear array of 70 stations equally spaced from 0.5° to 35° in epicentral distance from a nominal event location at a common azimuth. The resulting 70 × 70 covariance matrix then reveals the dependence of travel-time variance on distance and of travel-time correlation on distance and distance separation between stations. The calculations were done using travel-time sensitivities for the *ak135* 1D Earth model (Kennett et al., 1995), obtained with analytical solutions for geometrical rays (e.g., Buland and Chapman, 1983) and transformed to discrete sensitivities for a 3D model parameterization. The covariance matrix computations were performed with our explicit method.

We performed the calculations under two assumptions about the geostatistical parameters of velocity heterogeneity. In each, the correlation distances were the same as in the previous example (λ_1 = 300 km, λ_2 = 17.5 km in the crust and 60 km in the mantle). The standard deviation of velocity variations in the crust was also common to both cases: σ = 3% as before. The two geostatistical models differed in the velocity standard deviation assigned to the mantle. The first case used σ =1.5% throughout the mantle. The second case had σ = 2% in the upper mantle (above the

410-km discontinuity) and σ = 1% below 410 km. These parameters were chosen to illustrate the parameter dependence and are not necessarily indicative of the actual geostatistical properties of the Earth.

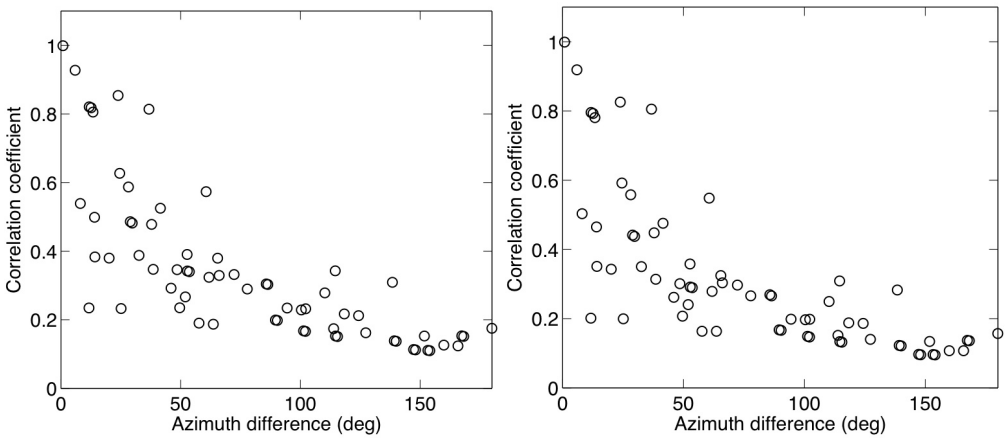

Figure 3. Correlation coefficient between model-errors as a function of azimuth difference between stations, computed with the explicit (left) and implicit (right) methods. The event-station geometry is shown in Figure 1.

Figure 4 shows the standard deviation of travel-time model errors for the two geostatistical models, each plotted versus epicentral distance. Distance-dependent discontinuities in the travel-time standard deviation are evident at the same distances in both models. These discontinuities are directly attributed to discontinuities in ray parameter, which are controlled by the *ak135* model. From approximately 2° to 15° travel-time error increases consistently, but not strictly linearly. The rate of increase in the error diminishes with distances, as rays begin to average over several correlation lengths of velocity variations. At approximately 15°, rays begin to dive deeper into the upper mantle and travel more vertically, resulting in more averaging over the shorter correlation-length anomalies in the vertical dimension. Several breaks in the error structure are evident as rays dive below the 410-km velocity discontinuity and then the 660-km discontinuity. Error structure stabilizes at teleseismic distances ($\geq$ 24°) when rays bottom in the lower mantle and the ray parameter remains continuous. Travel-time error is lower at teleseismic distance because vertically traveling rays in the more strongly heterogeneous upper mantle average over more wavelengths of geologic heterogeneity, recalling that we assumed the vertical scale of heterogeneity to be much smaller than the horizontal scale.

The travel-time error structure shown in Figure 4 is similar to that derived empirically (e.g., Flanagan et al., 2007). The similarity between empirical and our model-based predictions of travel-time error as a function of distance is encouraging. Further, these results provide insight into the non-intuitive but robust observation that teleseismic travel-time errors with long ray paths are smaller than regional travel-time errors with shorter ray paths.

Figure 5 shows the correlation matrix corresponding to the standard deviations shown in Figure 4. Analogous to the breaks in travel-time standard deviation, Figure 5 shows a roughly block-diagonal structure, with the blocks delimited by the same crossover distances and associated jumps in ray parameter. These results demonstrate that simple estimates of travel-time correlation based on the distance between stations do not adequately account for correlations between travel-times near crossover distances. If two stations straddle a break in ray parameter, then travel-time residuals are likely to be uncorrelated. This result has profound implications for both location algorithms and empirical methods (e.g., kriging) that make use of the travel-time residual covariance matrix.

CONCLUSIONS AND RECOMMENDATIONS

Our efforts to date confirm the feasibility of using a model-based approach to compute travel-time residual covariances. The numerical techniques we have developed are quite flexible in the station geometries and types of

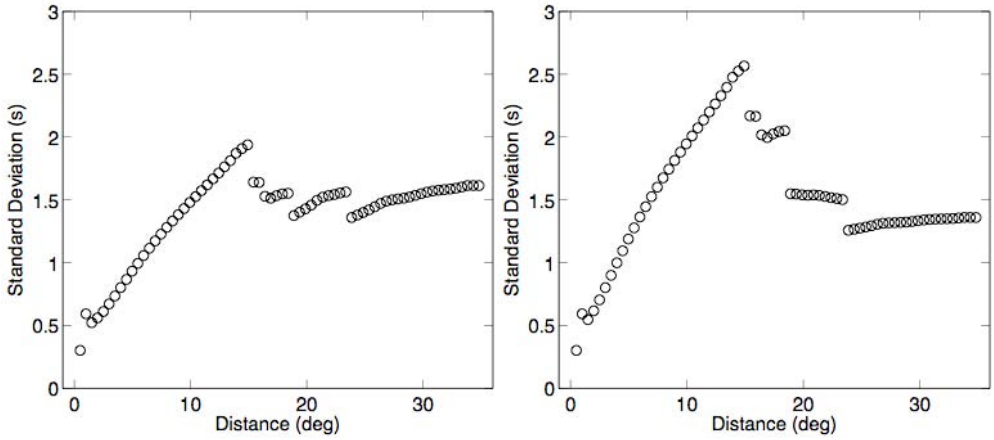

Figure 4. Standard deviation of travel-time model error as a function of epicentral distance computed with different geostatistical parameters for velocity heterogeneity. Both have a 3% velocity standard deviation (σ) in the crust. The results on the left correspond to σ = 1.5% everywhere in the mantle, while those on the right assign σ = 2% in the upper mantle above a depth of 410 km, and σ = 1% below 410 km. The same correlation lengths of heterogeneity were used in both cases (see text).

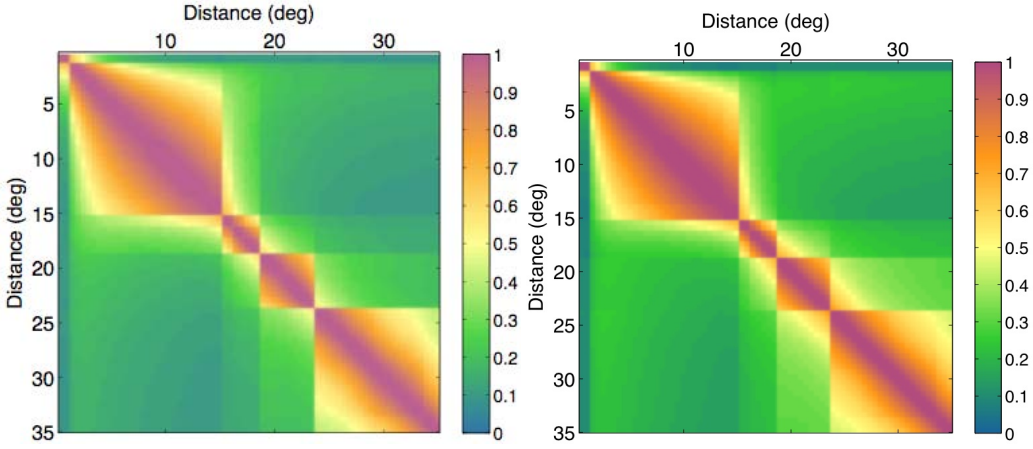

Figure 5. Correlation coefficient between model errors at different epicentral distances and a common azimuth, computed with the same two geostatistical models compared in Figure 4; σ = 1.5% throughout the mantle (left) and σ = 2% above 410 km and 1% below 410 km (right).

Earth models they can accommodate (1D and 3D), providing a useful tool for the theoretical investigation of how travel-time covariances behave in a variety of situations. Applying the techniques under even simple assumptions about the statistical properties of velocity anomalies in the Earth has already yielded important insights into previous empirical studies of travel-time residual structure as a function of epicentral distance (e.g. Myers and Schultz, 2000). Our approach goes beyond such studies by predicting details of the nonstationary correlations, which are difficult to resolve with empirical data but which are important to a seismic event locator. A crucial test of our approach will be location-validation experiments that quantify the location improvement one can achieve by using realistic travel-time covariance models.

REFERENCES

Buland, R., and C. H. Chapman (1983). The computation of seismic travel times, *Bull. Seism. Soc. Am.* 73: 1271–1302.

Chang, A. C., R. H. Shumway, R. R. Blandford and B. W. Barker (1983). Two methods to improve location estimates—preliminary results, *Bull. Seism. Soc. Am.* 73: 281–295.

Deutsch, C. V. and A. G. Journel (1998). *GSLIB: Geostatistical Software Library and User's Guide*, 2nd ed., Oxford University Press, Inc., New York, 369 pp.

Engdahl E. R., R. van der Hilst, and R. Buland (1998). Global teleseismic earthquake relocation with improved travel times and procedures for depth determination, *Bull. Seism. Soc. Am.* 88: 722–743.

Flanagan, M. P., S. C. Myers, and K. D. Koper (2007). Regional travel-time uncertainty and seismic location improvement using a three-dimensional a priori velocity model, *Bull. Seism. Soc. Am.* 97: 804–825.

Kennett, B. L. N., E. R. Engdahl, and R. Buland (1995). Constraints on the velocity structure in the Earth from travel times, *Geophys. J. Int.* 122: 108–124.

Myers, S. C., and C. A. Schultz (2000). Improving sparse network seismic locations with Bayesian kriging and teleseismically constrained calibration events, *Bull. Seism. Soc. Am.* 90: 199–211.

Reiter, D. and W. Rodi (2006). Crustal and upper-mantle P- and S-velocity structure in central and southern Asia from joint body- and surface-wave inversion, in *Proceedings of the 28th Seismic Research Review: Ground-Based Nuclear Explosion Monitoring Technologies*, LA-UR-06-5471, Vol. 1, pp. 209–218.

Rodi, W. L. and D. T. Reiter (2007). SAsia3d: A 3-D crust and upper-mantle velocity model of south Asia derived from joint inversion of P-wave travel times and surface-wave dispersion data, these Proceedings.

Rodi, W. and S. C. Myers (2006). Modeling travel-time correlations based on sensitivity kernels and correlated velocity anomalies, in *Proceedings of the 28th Seismic Research Review: Ground-Based Nuclear Explosion Monitoring Technologies*, LA-UR-06-5471, Vol. 1, pp. 475–483.

Rodi, W., S. C. Myers and C. A. Schultz (2003). Grid-search location methods for ground-truth collection from local and regional seismic networks, in *Proceedings of the 25th Seismic Research Review—Nuclear Explosion Monitoring: Building the Knowledge Base*, LA-UR-03-6029, Vol. 1, pp. 311–319.

Yang, X., I. Bondar, J. Bhattacharyya, M. Ritzwoller, N. Shapiro, M. Antolik, G. Ekstrm, H. Israelsson, and K. McLaughlin (2004). Validation of regional and teleseismic travel-time models by relocating ground-truth events, *Bull. Seism. Soc. Am.* 94: 897–919.